Where is the non-spin-flip isovector monopole resonance in ^{208}Tl?

G. Colò* and Nguyen Van Giai
Division de Physique Théorique, IPN, 91406 Orsay Cedex, France
(Received 10 January 1996)

The experimental study of the $\Delta T_z=+1$ component of the isovector monopole resonance of ^{208}Pb has revealed itself as an experimental puzzle. We present in this work a theoretical calculation of the strength distribution of this resonance and of its neutron decay properties, within the framework of a model in which random phase approximation states are coupled with continuum configurations and with a set of ''doorway states'' in order to describe the basic escape and damping mechanisms of the nuclear vibration. Our results are compared with existing measurements and with other theoretical analyses. [S0556-2813(96)03705-1]

PACS number(s): 21.10.Re, 21.60.Jz, 24.30.Cz, 27.80.+w

I. INTRODUCTION

Our knowledge of the properties of the isovector, non-spin-flip collective motion in atomic nuclei is still incomplete, as the large amount of experimental data and theoretical studies on the giant dipole resonance contrasts with the absence of systematics on other isovector multipole resonances. This is mainly because of the difficulties in finding selective probes which can excite these modes with sufficiently large cross sections. The simplest isovector non-spin-flip nuclear oscillation is the isovector giant monopole resonance (IVGMR) which has quantum numbers $L=0$, $S=0$, and $\Delta T=1$. The properties of this resonance are not yet fully clarified, despite their remarkable connection with interesting nuclear quantities such as the volume and surface symmetry energies of nuclear matter, or the isospin impurity in the ground state. Being also motivated by a renewed experimental interest [1] in the search for the $\Delta T_z=+1$ component of the IVGMR of ^{208}Pb which lies in the nucleus ^{208}Tl, we have performed a theoretical investigation of the decay properties of this resonance including its neutron emission. We are going to briefly review the present experimental situation on this subject before sketching the main characteristics of the theoretical model we have used and providing our set of results.

A first experiment aimed at identifying isovector charge-exchange resonances was performed on a series of targets with high-energy pions in Los Alamos by Erell *et al.* [2]. Even if the authors claimed that the (π^-,π^0) reaction on ^{208}Pb had given a signature of the IVGMR, this resonance appears (cf. Fig. 5 of [2]) as a very weak structure on a large background and its excitation energy with respect to the target ground state (12 MeV) must be compared with a nearly equal width (11.6 MeV). Then, it was pointed out that the (^{13}C, ^{13}N) reaction at incident energy of about 50 MeV/nucleon should populate strongly the non-spin-flip, isovector modes of the residual nucleus [3]. This reaction has therefore been performed on a set of nuclear targets at GANIL [4]. In almost all cases a wide resonance has been identified and its energy corresponds more or less to the same energy as the one found in Ref. [2]. But just in the case of ^{208}Tl the discrepancy between the two experiments is quite large, as the excitation energy measured in the (^{13}C, ^{13}N) reaction is 21.5 MeV (again with respect to the target ground state) and the width is 3.1 MeV. Besides that, some problems exist in the angular distributions which do not match exactly the expected behavior of a monopole excitation.

Finally, in a recent experiment [1] the reaction (^{13}C, ^{13}N) on the target ^{208}Pb was repeated at an energy of 60 MeV/nucleon and the neutron decay of the excited states in ^{208}Tl was measured. If the decay of the main peak is isotropic in the emitting nucleus reference frame, the identification of this peak as the IVGMR can be given more support. The result of the experiment is a confirmation of the findings by [4]: A peak at 21.5 MeV has been found, but still the angular distribution does not fit with the calculations performed for a $L=0$ state. The percentage of direct decay of this peak is reported to be about 22% but this result is obtained without a statistically significant angular distribution and this fact prevents one from saying that an unambigous signature of the $L=0$ character of the observed resonance has been found. On the other hand, this is the first attempt to measure the neutron decay of the charge-exchange IVGMR and the experiment is continuing on ^{208}Pb as well as on other targets. It is therefore very useful to have for the first time a theoretical calculation of this decay.

II. THEORY

In previous works we have already calculated the neutron decay of the isoscalar giant monopole resonance [5] and the proton decay of the isobaric analog and Gamow-Teller resonances [6]. The latter results of Ref. [6] are in a general satisfactory agreement with recent experimental data [7] so that we can be confident about our method of calculation of the particle decay of giant resonances. This method is based on a microscopic model of collective nuclear excitations in which random phase approximation (RPA) states are coupled to ''doorway states'' composed of one-particle–one-hole (1p-1h) configurations plus a low-lying collective vibration, and to 1p-1h continuum states. The two couplings are intended to describe the essential physical mechanisms leading to the spreading of the collective mode and to its decay by particle emission, respectively. We use an effective interac-

*Present address: Dipartimento di Fisica, Università degli Studi, via Celoria 16, 20133 Milano, Italy.

tion of the Skyrme type throughout the whole calculation, and so the model has the advantage of being self-consistent and has no free parameters. We will give a brief outline of the model in the following and refer the reader to Ref. [6] for a detailed explanation of it.

We start by solving the Hartree-Fock (HF) set of equations in coordinate space for a given nucleus (A,Z). The self-consistent mean field is then diagonalized on a basis made up with harmonic oscillator wave functions and a finite set of occupied and unoccupied levels labeled by $|i\rangle$ is thus determined. In the case at hand, 15 harmonic oscillator shells with $\hbar\omega = 6.2$ MeV have been used to diagonalize the mean field. Let us call Q_1 the subspace of nuclear configurations made of 1p-1h excitations built within the set $|i\rangle$. Subspaces and projectors will be denoted by the same symbol in the following. The nuclear Hamiltonian restricted to Q_1 can be written as

$$Q_1 H Q_1 = Q_1 (H_0 + V_{\rm ph}) Q_1, \tag{2.1}$$

where H_0 is the HF Hamiltonian and $V_{\rm ph}$ is the particle-hole interaction determined as the functional derivative of the mean field with respect to the density. The RPA eigenstates of the Hamiltonian (2.1) will be denoted by $|n\rangle$.

In order to account for escape and spreading effects, we build two other orthogonal subspaces P and Q_2. The space P is made up of particle-hole configurations where the particle is in a continuum state orthogonal to all states $|i\rangle$. To determine these unbound states, we use the procedure of [8]. The space Q_2 is built with a set of ''doorway states,'' the first step in the coupling of the ordered resonance motion with the compound nuclear states, and we denote these ''doorway states'' by $|N\rangle$. Like in previous studies [5,6] we make the physical choice of describing them as states made up with discrete 1p-1h configurations coupled to a collective vibration. The collective vibrations are chosen among the RPA states $|n\rangle$ mentioned above. The significance of the present choice is that only a few collective states participate effectively to the spreading mechanism [9].

Using the technique described in [10] one can show that the coupling of the eigenstates of the Hamiltonian (2.1) with the configurations belonging to P and Q_2 can be taken into account by diagonalizing the effective Hamiltonian

$$\begin{aligned}\mathscr{H}(\omega) &\equiv Q_1 H Q_1 + W^{\uparrow}(\omega) + W^{\downarrow}(\omega)\\ &= Q_1 H Q_1 + Q_1 H P \frac{1}{\omega - PHP + i\epsilon} P H Q_1\\ &\quad + Q_1 H Q_2 \frac{1}{\omega - Q_2 H Q_2 + i\epsilon} Q_2 H Q_1,\end{aligned} \tag{2.2}$$

where ω is the excitation energy. This energy-dependent Hamiltonian has complex eigenvalues whose imaginary parts originate from coupling to unbound and to more complicated configurations and are related to escape and spreading widths.

The escape term $W^{\uparrow}(\omega)$ can be easily evaluated if one replaces the complete Hamiltonian H by its one-body part H_0. This approximation has been checked independently by various authors [11,12] and it is found to be a valid assumption. The matrix elements of the spreading term $W^{\downarrow}(\omega)$ on a basis of Q_1 can also be determined in a straightforward way if we make the ansatz that the states $|N\rangle$ of Q_2 are not interacting (cf. Appendix A of Ref. [6] for details).

To solve the effective Hamiltonian (2.2) it is convenient to work in the basis of the RPA states $|n\rangle$. The eigenvalue equation for the effective Hamiltonian (2.2) can then be cast in matrix form [6]. We shall denote by $\Omega_\nu - i\Gamma_\nu/2$ its eigenvalues and by F the matrix of the corresponding eigenvectors $|\nu\rangle$ according to

$$|\nu\rangle = \sum_n F_n^{(\nu)} |n\rangle. \tag{2.3}$$

In terms of these quantities the response function corresponding to a given operator O and the related strength distribution are

$$R(\omega) = \sum_\nu \langle 0|O|\nu\rangle^2 \frac{1}{\omega - \Omega_\nu + i\dfrac{\Gamma_\nu}{2}}, \tag{2.4}$$

$$S(\omega) = -\frac{1}{\pi} \mathrm{Im} R(\omega). \tag{2.5}$$

Interesting quantities which can be extracted from the model and which are actually measured in the particle decay experiments are the branching ratios B_c corresponding to particular decay channels. An escaping nucleon with energy ε leaves a residual $(A-1)$ system in a hole state such that by energy conservation $\varepsilon_h = \varepsilon - \omega$, where ω is the initial excitation energy. The cross section σ_c for this decay as well as the excitation cross section $\sigma_{\rm exc}$ can be easily evaluated in plane wave Born approximation [8]. The branching ratio comes out as

$$\begin{aligned}B_c \equiv \frac{\sigma_c}{\sigma_{\rm exc}} = \pi i \sum_{\nu,\nu'} &\frac{\gamma_{\nu\nu',c} S_{\nu\nu'}}{(\omega_{\nu'} - \omega_\nu) + \dfrac{i}{2}(\Gamma_{\nu'} + \Gamma_\nu)}\\ &\times \left(\sum_{\nu,\nu'} (F^* F^T)_{\nu\nu'} S_{\nu\nu'} \right)^{-1},\end{aligned} \tag{2.6}$$

where

$$S_{\nu\nu'} \equiv \langle \nu|O|0\rangle \langle \nu'|O|0\rangle^* \tag{2.7}$$

and

$$\gamma_{\nu\nu',c} = \int d\Omega_k \langle \varphi_c u_{c,\varepsilon}^{(-)}(\vec{k})|H_0|\nu\rangle \langle \varphi_c u_{c,\varepsilon}^{(-)}(\vec{k})|H_0|\nu'\rangle^*. \tag{2.8}$$

In this equation φ_c is the wave function describing the residual $(A-1)$ nucleus in channel c, and $u_{c,\varepsilon}^{(-)}(\vec{k})$ is the escaping particle wave function belonging to P space.

III. RESULTS AND DISCUSSION

The operator which excites the IVGMR is

$$O_\mu = \sum_i r_i^2 t_\mu{}^{(i)}, \tag{3.1}$$

where $\mu = 0, \pm$. The $\mu = \pm$ components must be treated at the same time within the framework of the charge-exchange RPA [13]. We have therefore worked within a space Q_1 made up with 132 proton-particle–neutron-hole configurations and 96 neutron-particle–proton-hole configurations and obtained the RPA spectrum for the excitation of the two components, respectively, in ^{208}Bi and ^{208}Tl. The following sum rule, i.e., the sum of the energy-weighted sum rules for the operators O_- and O_+, holds in the charge-exchange RPA with Skyrme-type interactions [13]:

$$m_1(O_-) + m_1(O_+) = \frac{2\hbar^2}{m} A\langle r^2\rangle(1+\kappa+\eta), \tag{3.2}$$

where

$$\kappa = \frac{\left[t_1\left(1+\frac{x_1}{2}\right)+t_2\left(1+\frac{x_2}{2}\right)\right]\int d^3r r^2 \rho_n(\vec{r})\rho_p(\vec{r})}{\hbar^2 A\langle r^2\rangle/2m} \tag{3.3}$$

and

$$\eta = \frac{\frac{1}{2}\left[t_1\left(1+\frac{x_1}{2}\right)+t_2\left(1+\frac{x_2}{2}\right)\right]\int d^3r r^2[\rho_n(\vec{r})-\rho_p(\vec{r})]^2 + \int d^3r r^4 V_{\rm Coul}(\vec{r})[\rho_n(\vec{r})-\rho_p(\vec{r})]}{2\hbar^2 A\langle r^2\rangle/m}. \tag{3.4}$$

The t_i and x_i are interaction parameters and $V_{\rm Coul}$ is the HF one-body Coulomb potential whereas ρ_n and ρ_p are HF neutron and proton densities, respectively [notice a misprint in Eq. (65) of [13] which is inconsistent with Eq. (46) of the same paper]. We have performed calculations with the two Skyrme forces SIII and SGII which have been shown to give reasonable energies in RPA for the $\mu=0$ component of the IVGMR in ^{208}Pb [14] and in both cases with our choice of the 1p-1h space the RPA results exhaust essentially all the sum rule (3.2).

If we solve in the RPA the Hamiltonian (2.2) without the term $W^{\downarrow}(\omega)$, our procedure should be equivalent to the continuum RPA of [13]. Indeed, the results we have obtained with the force SIII agree rather well with the findings of Ref. [13]. We have then built the configurations of Q_2 by means of the p-h states of the space Q_1 and the isoscalar phonons of ^{208}Pb with multipolarity $L \leqslant 4$ and energy smaller than 20 MeV (see [6] where more details about this set of collective states are provided). When building the matrix elements of $W^{\downarrow}(\omega)$, a finite averaging parameter Δ has been used instead of the infinitesimal ϵ which appears in the last term of Eq. (2.2). The value $\Delta = 0.5$ MeV is adopted and we have checked the stability of the results when Δ is varied around this value. We have solved the complete Hamiltonian (2.2) for the experimentally relevant $\mu = +$ component [we also stress that in this neutron-particle–proton-hole channel the isospin of excited states built on the $T_0 = (N-Z)/2$ ground state of ^{208}Pb is well defined as T_0+1 and one does not have to perform any isospin projection]. The resulting strength distribution [see Eq. (2.5)] calculated up to 30 MeV (we always refer to excitation energies in ^{208}Tl calculated with respect to ^{208}Pb ground state) exhausts about 90% of the energy-weighted sum rule found in the RPA 1p-1h calculation, the obtained values being 1.13×10^5 (1.03×10^5) MeV fm^4 in the case of the interaction SIII (SGII), to be compared with 1.26×10^5 (1.10×10^5) MeV fm^4 for 1p-1h RPA. The strengths calculated with SIII and SGII are depicted in Fig. 1. In the same figure is shown the singles spectrum from the (^{13}C, ^{13}N) reaction [1] where the background has been subtracted. This background due to pickup-breakup processes and quasifree charge-exchange reactions is large but smooth. In the experimental spectrum one can see some small structures at 9 and 13 MeV, and a larger structure at 21 MeV. The latter is conjectured to be of $L=0$ nature although the evidence from angular distributions is far from compelling.

Let us first discuss the position of the peaks. In Table I are shown peak energies calculated by different authors. An interesting feature is that the same interaction SIII has been used in Refs. [13,15] and in the present work but the results show some variations due to the different models used. The value 17.2 MeV of Ref. [13] comes from a continuum-RPA calculation where no spreading effect is included. The model of Ref. [15] contains a 2p-2h spreading mechanism which is quite effective in widening the peak but the authors simply dropped the real part of the corresponding $W^{\downarrow}$ and thus they missed a downward shift of about 1 MeV. Furthermore, the coupling to the continuum is not taken explicitly into account in Ref. [15] and this explains for the 1.8 MeV difference between Refs. [13] and [15]. Finally, the present result of 16.2 MeV obtained with SIII includes the downward shifts caused by continuum coupling and coupling to doorway states. This leaves us with a rather large discrepancy of 5 MeV if we compare with experiment. Even worse, this discrepancy would be increased by another 3 MeV if one uses interaction SGII. It must be noted again that both interactions SIII and SGII are doing reasonably well in the non-charge-exchange channel, i.e., for the isovector monopole resonance in ^{208}Pb [14]. In the absence of a clear experimental signature of the $L=0$ nature of the peak at 21 MeV one may wonder if other multipolarities may exist at that energy. Earlier RPA calculations with the interaction SIII [13] have indicated that $L=1$ and $L=2$ strengths are concentrated at

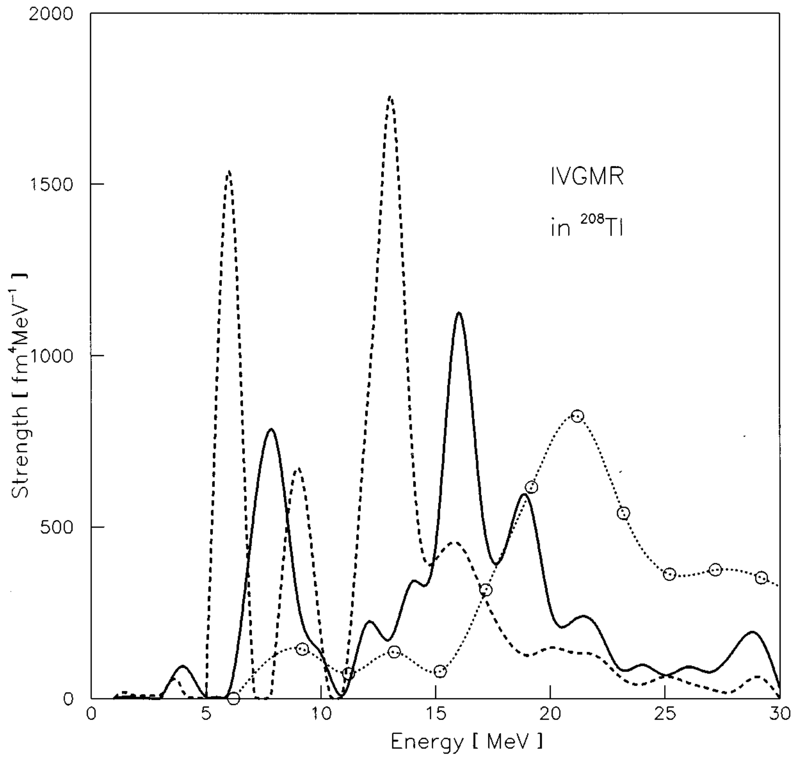

FIG. 1. Strength distribution of the isovector monopole resonance in ^{208}Tl. The solid (dashed) line corresponds to the results calculated with SIII (SGII) interaction. The open circles are the singles spectrum of Ref. [1] (in arbitrary scale) with subtracted background. The thin dashed line which connects the circles has been drawn to guide the eye.

lower energies, below 10 and 15 MeV, respectively. We have calculated the $L=3$ RPA strength distributions and we have found that in the 20 MeV region the interactions SIII and SGII predict about 20% and 15% of non-energy-weighted octupole strength, respectively. Thus, it cannot be excluded that the experimental peak at 21 MeV contains some amount of $L=3$ strength.

We come now to the width of the IVGMR. In our model, the total width contains both escape and spreading mechanisms and it turns out that it is less dependent on the effective interaction than the position of the state. For SIII and SGII the full width at half maximum of the high-lying peak is about 1.8 MeV. In fact, a number of substructures are present in the distributions which look rather spread out. If we parametrize the main peak and the shoulders or secondary peaks around it with a single Gaussian or Lorentzian function, we find a larger value for the total width, i.e., between 3 and 5 MeV. This compares well with the total width of 4.2 MeV calculated in [15], where the coupling of the main IVGMR peak with 2p-2h ‘‘doorway states’’ has been considered and the escape width was added by assuming that the escape term $W^{\uparrow}(\omega)$ is independent of energy. Finally, we have indicated for completeness in Table I the value $\Gamma^{\uparrow}=1.9$ MeV obtained in the continuum-RPA [13], but of course, this quantity represents only the escape width and some Landau damping width.

An interesting feature of our calculated strength distributions is the secondary structure at low energy: a single peak in the case of the force SIII and a double bump in the case of the force SGII. In order to gain more insight into the microscopic structure of these peaks we have calculated the transition densities of the main states contributing to the peaks. The complex transition density of the eigenstate $|\nu\rangle$ of the effective Hamiltonian (2.2) is defined as

$$\delta\rho_{\nu}(r)=\sum_{n} F_n^{(\nu)}\delta\rho_n(r), \tag{3.5}$$

where the coefficients $F_n^{(\nu)}$ are defined by Eq. (2.3) and the transition densities of the RPA eigenstates $|n\rangle$ are

TABLE I. Excitation energy E and width Γ of the IVGMR in ^{208}Tl (all values are in MeV). The energy is with respect to the ground state of the parent nucleus ^{208}Pb and it is 4.2 MeV higher than the energy with respect to the ground state in ^{208}Tl.

	Experiment		Theory			
	Ref. [2]	Refs. [1,4]	Ref. [13]	Ref. [15]	This work SIII	This work SGII
E (high peak)	11.2± 2.8	20.7 ± 0.6	17.2	19.0	16.2	13.2
(low peaks)					(7.8)	(6.0, 9.0)
Γ	11.6	3.1	~ 1.9[a]	4.2	~ 4.0[b]	

[a]This value was obtained in the continuum-RPA but contains no spreading width.

[b]See the text for a discussion about extracting a width from our strength distributions.

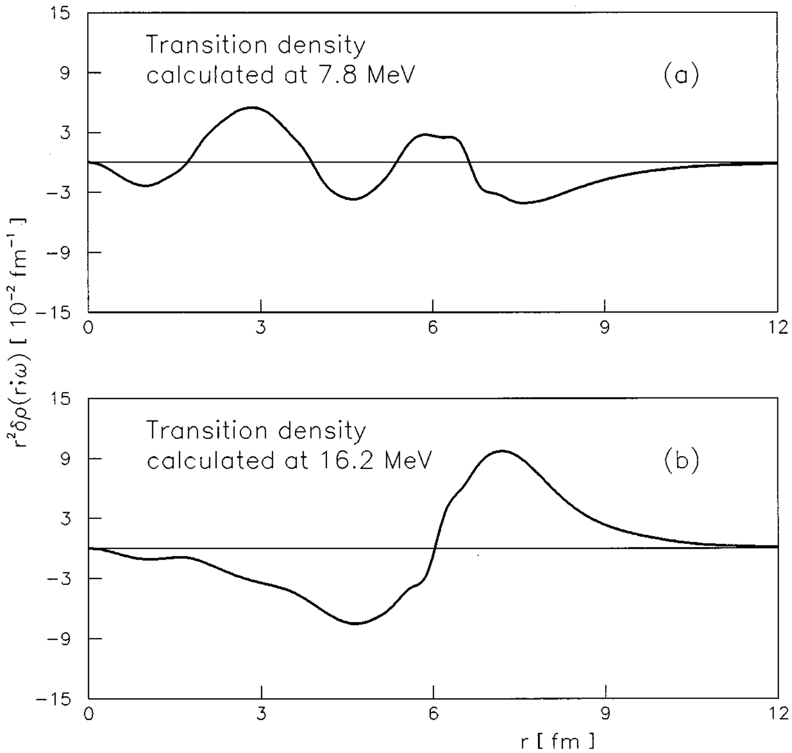

FIG. 2. Transition densities $r^2\delta\rho(r;\omega)$ calculated with interaction SIII. The energies ω correspond to the low-energy peak at 7.8 MeV (upper part) and the high-energy peak at 16.2 MeV (lower part).

$$\delta\rho_n(r)=\sum_{\mathrm{ph}}(X_{\mathrm{ph}}^{(n)}-Y_{\mathrm{ph}}^{(n)})\langle \mathrm{p}||Y_L||\mathrm{h}\rangle R_{\mathrm{p}}(r)R_{\mathrm{h}}(r). \quad (3.6)$$

In the above equation L is the multipolarity of the RPA state, ph labels its particle-hole components, and $R_i(r)$ is the radial part of the single-particle wave function of state i. From the structure of Eqs. (2.4), (2.5) one can easily identify the Green's function $G(\vec{r},\vec{r}\,';\omega)$ and hence the (real) transition density $\delta\rho(r;\omega)$ at energy ω defined through

$$|\delta\rho(r;\omega)|^2=-\frac{1}{\pi}\mathrm{Im}\sum_{\nu}[\delta\rho_{\nu}(r)]^2\frac{1}{\omega-\Omega_{\nu}+\dfrac{i\Gamma_{\nu}}{2}}. \quad (3.7)$$

We have checked that the continuum-RPA transition densities of [13] are recovered within the present approach when calculations are performed without $W^{\downarrow}$ and using the interaction SIII. This fact is further confirmation of the accuracy of our method of treating the coupling with continuum states. In Fig. 2 we show the transition densities $r^2\delta\rho(r;\omega)$ calculated with the full Hamiltonian (2.2), at energies ω corresponding to the low-lying and high-lying peaks. The shape of the high-energy transition density is typical of a collective mode with only one node in the surface region. It is interesting to note that the radial shape of the transition density of this collective state is practically the same if we calculate with $W^{\uparrow}$ only or with $W^{\uparrow}+W^{\downarrow}$; i.e., damping effects do not affect the shape of the collective transition density. On the other hand, the low-energy transition density has many nodes and the inner region around 3 fm contributes importantly. This could result in a difference of relative excitation cross sections for the upper and lower peaks depending on the nature of the incoming projectile, the low-energy peak being more easily excited by pions than by heavy ions since the latter projectiles are more absorbed at the nuclear surface. The calculated strength distributions seem to contain both the peak which has been seen by means of pion charge exchange and the higher peak which appears in the (^{13}C, ^{13}N) reaction since the difference between the two experimental values is comparable with the difference between the energy of the high- and low-energy structures (see Table I).

Finally, we have extracted the branching ratios of neutron decay leading to the valence proton-hole states of ^{207}Tl by averaging the numerator and the denominator of Eq. (2.6) in the interval 13–19 MeV (11–16 MeV) for the case of the force SIII (SGII). The obtained values are collected in Table II. Like the total widths, they are not too markedly dependent on the particular Skyrme interaction. The sum of the branching ratios corresponds to a fraction of direct decay of about 0.4–0.5 with the largest contribution coming from the $h_{11/2}$ channel. Experimentally, it is found that the peak at 20.7 MeV has a branching ratio of direct neutron decay of 0.22 [1] which is about half of the theoretical prediction. If we

TABLE II. Branching ratios B_c for the neutron decay of the IVGMR leaving the residual nucleus ^{207}Tl in a valence proton hole state c.

Decay channel	Hole energies (MeV) HF(SIII)	HF(SGII)	Expt.	Branching ratios SIII	SGII
$s_{1/2}$	-7.95	-7.29	-8.01	0.043	0.037
$d_{3/2}$	-8.52	-7.67	-8.36	0.032	0.028
$h_{11/2}$	-9.66	-7.80	-9.35	0.254	0.256
$d_{5/2}$	-10.28	-9.26	-10.5	0.111	0.053
$g_{7/2}$	-13.59	-12.06	-12.0	0.067	0.052
$\Sigma_c B_c$				0.507	0.426

renormalize the final hole states by means of empirical spectroscopic factors taken from [16], the sum of the branching ratios becomes 0.331 and 0.262 for interactions SIII and SGII, respectively, i.e., not so far from the experimental value. It would be interesting if future neutron decay experiments of the IVGMR could measure branching ratios to specific final states so that one can compare further the data with predictions of models. We have also checked the sensitivity of these branching ratios to the energy position of the IVGMR peak. If we artificially move up or down this energy by an amount of 2 MeV, the sum of the branching ratios varies by about 20%.

IV. CONCLUSION

Motivated by the contradictory experimental results of pion-induced and heavy-ion-induced charge-exchange reactions on ^{208}Pb we have performed a microscopic calculation of the non-spin-flip IVGMR in ^{208}Tl. We use a model which can describe both escape and damping effects and which was shown previously to work reasonably well for isobaric analog and Gamow-Teller resonances within the uncertainties linked to the effective interactions. In the present work we give predictions about the position, total width, and partial neutron escape widths of the IVGMR in ^{208}Tl based on two often used effective interactions, the Skyrme forces SIII and SGII. The first observation is that the predicted position of the IVGMR depends on the particular effective interaction, the variation being as much as 3 MeV between the two interactions used. None of them agrees with the position of the main bump observed in (^{13}C, ^{13}N) reactions. If the energy of the IVGMR is experimentally confirmed this would raise an interesting problem about effective interactions. In order to obtain this information, it would be desirable to disentangle experimentally the $L=0$ strength from other multipolarities. Our RPA calculations indicate that a non-negligible fraction of $L=3$ strength is in the region of the experimentally observed bump.

On the other hand, the total width and partial neutron widths are much less sensitive to the interaction used. It would be interesting to measure partial escape widths in order to make more detailed comparisons with the theoretical predictions.

Finally, the microscopic model also predicts the existence of noncollective, low-lying states around 8 MeV. These states might correspond to the states observed in the early (π^-,π^0) experiments. In the recent (^{13}C, ^{13}N) experiments there are also indications of structures in this energy region.

ACKNOWLEDGMENTS

We thank I. Lhenry for discussions on the (^{13}C, ^{13}N) measurements. One of us (G.C.) would like to acknowledge the financial support of the European Community (Contract No. CHRXCT92-0075), as well as the very nice hospitality of the Division de Physique Théorique of the IPN where this work has been carried out. DPT-IPN Orsay is a Unité de Recherche des Universités Paris XI et Paris VI associée au CNRS.

[1] I. Lhenry *et al.*, Nucl. Phys. **A583**, 115 (1995); I. Lhenry, Nucl. Phys. A (to be published).
[2] A. Erell, J. Alster, J. Lichtenstadt, M.A. Moinester, J.D. Bowman, M.D. Cooper, F. Irom, H.S. Matis, E. Piasetzky, and U. Sennhauser, Phys. Rev. C **34**, 1822 (1986).
[3] C. Bérat, M. Buénerd, J. Chauvin, J.Y. Hostachy, D. Lebrun, P. Martin, J. Barrette, B. Berthier, B. Fernandez, A. Miczaïka, W. Mittig, E. Stiliaris, W. von Oertzen, H. Lenske, and H.H. Wolter, Phys. Lett. B **218**, 299 (1989).
[4] C. Bérat, M. Buénerd, J.Y. Hostachy, P. Martin, J. Barrette, B. Berthier, B. Fernandez, A. Miczaïka, A. Villari, H.G. Bohlen, S. Kubono, E. Stiliaris, and W. von Oertzen, Nucl. Phys. **A555**, 455 (1993).
[5] G. Colò, P.F. Bortignon, Nguyen Van Giai, A. Bracco, and R.A. Broglia, Phys. Lett. B **276**, 279 (1992).
[6] G. Colò, Nguyen Van Giai, P.F. Bortignon, and R.A. Broglia, Phys. Rev. C **50**, 1496 (1994).
[7] H. Akimune, I. Daito, Y. Fujita, M. Fujiwara, M.B. Greenfield, M.N. Harakeh, T. Inomata, J. Jänecke, K. Katori, S. Nakayama, H. Sakai, Y. Sakemi, M. Tanaka, and M. Yosoi, Phys. Lett. B **323**, 107 (1994).
[8] S. Yoshida and S. Adachi, Z. Phys. A **325**, 441 (1986).
[9] G.F. Bertsch, P.F. Bortignon, and R.A. Broglia, Rev. Mod. Phys. **55**, 287 (1983).
[10] S. Yoshida, Suppl. Prog. Theor. Phys. **74&75**, 142 (1983).
[11] N. Van Giai, P.F. Bortignon, F. Zardi, and R.A. Broglia, Phys. Lett. B **199**, 155 (1987).
[12] S. Yoshida and S. Adachi, Nucl. Phys. **A457**, 84 (1986).
[13] N. Auerbach and A. Klein, Nucl. Phys. **A395**, 77 (1983).
[14] G. Colò, N. Van Giai, and H. Sagawa, Phys. Lett. B **363**, 5 (1995).
[15] S. Adachi and N. Auerbach, Phys. Lett. **131B**, 11 (1983).
[16] C. Mahaux and R. Sartor, Adv. Nucl. Phys. **20**, 1 (1991).